

Unified model for non-Abelian braiding of Majorana and Dirac fermion zero modes

Tianyu Huang,^{1,*} Rui Zhang,^{2,*} Xiaopeng Li,^{3,4,5} Xiong-Jun Liu,^{2,6,7,†} X. C. Xie,^{1,2,7,‡} and Yijia Wu^{1,3,7,§}

¹*Interdisciplinary Center for Theoretical Physics and Information Sciences, Fudan University, Shanghai 200433, China*

²*International Center for Quantum Materials, School of Physics, Peking University, Beijing 100871, China*

³*State Key Laboratory of Surface Physics and Institute for Nanoelectronic Devices and Quantum Computing, Fudan University, Shanghai 200433, China*

⁴*Department of Physics, Fudan University, Shanghai 200433, China*

⁵*Shanghai Qi Zhi Institute, AI Tower, Xuhui District, Shanghai 200232, China*

⁶*International Quantum Academy, Shenzhen 518048, China*

⁷*Hefei National Laboratory, Hefei 230088, China*

(Dated: October 10, 2024)

Majorana zero modes (MZMs) are the most intensively studied non-Abelian anyons. The Dirac fermion zero modes in topological insulators can be interpreted as the symmetry-protected “doubling” of the MZMs, suggesting an intrinsic connection between the quantum statistics of the two types of zero modes. Here we find that the minimal Kitaev chain model provides a unified characterization of the non-Abelian braiding statistics of both the MZMs and Dirac fermion zero modes under different parameter regimes. In particular, we introduce a minimal tri-junction setting based on the minimal Kitaev chain model and show it facilitates the unified scheme of braiding Dirac fermion zero modes, as well as the MZMs in the assistance of a Dirac mode. This unified minimal model unveils that the non-Abelian braiding of the MZMs can be continuously extended to the realm of Dirac fermion zero modes. The present study reveals deeper insights into the non-Abelian statistics and enables a broader search for non-Abelian anyons beyond the scope of MZMs.

Introduction. Anyons [1] obeying fractional statistics are exotic quasiparticles living in (2+1)-dimensional space. In condensed matter physics, anyons usually emerge as composites formed from charged particles (like electrons) and vortices. This anyon model was raised by Wilczek in 1982 [1] and first exemplified by the Laughlin quasiparticles [2] in the fractional quantum Hall (FQH) system [3]. Also in the $\nu = 5/2$ FQH state [4], the more intriguing non-Abelian anyons are proposed to emerge as the elementary excitations binding with half-vortices [5, 6]. This type of excitation in correlated electron systems also manifests itself as a half-vortex-bound state in p -wave superconductors [7], which is well known as the Majorana zero mode (MZM) [8].

Following these pioneering works, great efforts have been devoted to seeking the experimental evidence of MZMs because of their great potential for fault-tolerant topological quantum computation [9, 10]. MZMs have been proposed to appear in a number of platforms, an incomplete list includes superconductor-semiconductor heterostructures [11–14], ferromagnetic atomic chains on a superconductor [15], and vortices in topological superconductors [16–19]. However, the complexity of the superconductor-proximate heterostructure [14, 20] as well as the possible trivial explanations for the transport signals [21, 22] still hinder the appearance of the smoking-gun experimental signals. An alternative way is to seek the symmetry protected Majorana pairs. The most studied one among them is the Majorana Kramer’s pair (MKP) [23, 24], where a pair of MZMs is related by time-reversal (TR) symmetry. Owing to the TR symmetry protection, MKPs have been shown to obey non-Abelian braiding, rendering a novel type of symmetry-

protected non-Abelian statistics [25–28], as well as topological quantum computing [29].

When the TR symmetry (an anti-unitary symmetry) in the MKP is replaced by a unitary symmetry, the symmetry-protected non-Abelian statistics remains [30]. This kind of Majorana pair related by a unitary symmetry is equivalent to a zero-energy Dirac fermion mode bound to a half vortex [31, 32], and the proof of the non-Abelian statistics for Dirac fermion modes can be traced back to Yasui et al.’s work in 2012 [32]. This kind of zero-energy Dirac fermion mode can appear as a bound state with a half-vortex attached in a two-dimensional topological insulator [33]. The incarnation of this non-Abelian Dirac fermion zero mode in one-dimensional system is the celebrated Jackiw-Rebbi zero mode, whose half-integer fractional charge [34, 35] and non-Abelian braiding [36–38] have been discussed in the early works.

The fact that the Dirac fermion zero modes obeying non-Abelian braiding statistics can be understood in the following way. Given the presence of a unitary symmetry, a set of Dirac fermion zero modes can be decomposed into two sets of MZMs in which the cross coupling between the opposite sets is prohibited by symmetry. Therefore, the braiding of Dirac fermion modes can be characterized as the direct product of the braiding of two sets of MZMs [30]. In this way, the non-Abelian braiding statistics of the Dirac fermion zero modes are essentially related to the pairs of MZMs. In addition, it has long been discussed that the braiding operation of MZMs can be facilitated by a Dirac fermion zero mode, which is known as the “quantum-dot (QD)-assisted Majorana braiding” [39–43]. In this braiding scheme, the low-lying states involved include both the MZMs and Dirac fermion modes.

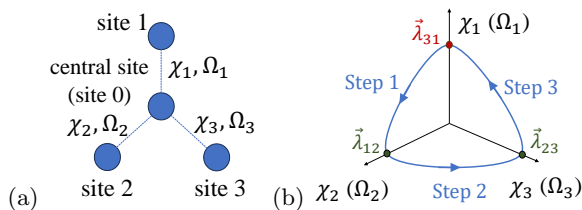


FIG. 1: (a) Sketch of the Y-junction jointed by minimal Kitaev chains. (b) The braiding operation corresponds to a closed loop (started and ended at the point marked in red) in the parameter space.

The presence of such braiding scheme intermediating between the Majorana and the Dirac fermionic systems further hints us that these braiding schemes mentioned above might be described in a unified model.

In this Letter, we demonstrate that the minimal Kitaev chain model [44, 45] can play this role. To be specific, under different parameter choices, the minimal Kitaev chain can depict the non-Abelian braiding of MZMs, Dirac fermion zero modes, as well as the QD-assisted Majorana braiding. Significantly, the quasiparticles being braided in our setting can switch from the MZMs to Dirac fermion zero modes with a small change in parameters. It indicates that the search for non-Abelian anyons shall not be confined to the realm of MZMs. In fact, the degenerate Dirac fermion zero modes can always be regarded as the symmetry protected “doubling” of the MZMs [30, 46]. In addition to providing new insights into non-Abelian anyons, our proposed study based on minimal Kitaev chain model is experimentally feasible and could be detected using ultracold atoms or QD arrays.

Braiding in minimal Kitaev chain. The celebrated Kitaev’s chain [8] model supports MZMs as its topological edge states. The two-site version of the Kitaev’s chain is known as the minimal Kitaev chain [44, 45], which can be described by $H = \chi d_L^\dagger d_R + \Omega d_L^\dagger d_R^\dagger + \text{h.c.}$. Here, the index L (R) denotes the left (right) site. It is worth noting that, despite lacking a continuous k -space, the minimal Kitaev chain can still be depicted by a \mathbb{Z}_2 topological index [8, 47–49] through the Pfaffian of the Hamiltonian in the Majorana basis at momentum $k = 0$ and $k = \pi$. The minimal Kitaev chain reaches the “sweet spot” [45] when the hopping amplitude χ is equal to the superconducting pairing amplitude Ω and both of them are real numbers ($\chi = \Omega \in \mathbb{R}$, where the Hamiltonian above reduces to $H = -i|\chi| \cdot i(d_L^\dagger - d_L)(d_R + d_R^\dagger)$). In this way, two isolated MZMs appear at the left and the right site as $(d_L + d_L^\dagger)$ and $i(d_R^\dagger - d_R)$, respectively, which are termed poorman’s MZMs (PMMs) [44, 45].

However, properly defining non-Abelian braiding requests at least four MZMs [7]. Therefore, in order to perform the braiding of the PMMs, the minimal device required is a four-site Y-shaped junction [50–52] jointed

	$\theta_{\chi_j}, \theta_{\Omega_j} = 0$	$\theta_{\chi_j}, \theta_{\Omega_j} \neq 0$
$ \chi_j = \Omega_j $	Case I: poorman’s MZMs (PMMs)	Case II: QD-assisted MZM braiding
$ \chi_j \neq \Omega_j $	Case III: Dirac fermion zero modes (unitary-symmetry preserved)	Case IV: Dirac fermion zero modes (unitary-symmetry broken)

TABLE I: The minimal-Kitaev-chain-based Y-junction can depict the non-Abelian braiding of different types of low-lying modes depending on the choices of χ ’s and Ω ’s.

by three minimal Kitaev chains [see Fig. 1(a)]

$$H = \sum_{j=1}^3 \chi_j d_0^\dagger d_j - \chi_j^* d_0 d_j^\dagger + \Omega_j d_0^\dagger d_j^\dagger - \Omega_j^* d_0 d_j. \quad (1)$$

Here, d_j (d_j^\dagger) annihilates (creates) an electron on site j , while d_0 (d_0^\dagger) annihilates (creates) an electron on the central site, χ_j and Ω_j are the amplitudes of the hopping and superconducting pairing, respectively. In general, χ ’s and Ω ’s are complex as $\chi_j = |\chi_j|e^{i\theta_{\chi_j}}$ and $\Omega_j = |\Omega_j|e^{i\theta_{\Omega_j}}$. Significantly, it is impossible to gauge away all these six phases θ_{χ_j} and θ_{Ω_j} ($j = 1, 2, 3$), since in Eq. (1), there are only four electron operators can be utilized to absorb the gauge phases. In other words, the “sweet spot” condition cannot always be satisfied when we consider the braiding in this minimal-Kitaev-chain-based Y-junction. Nonetheless, the non-Abelian braiding physics shall not collapse due to a slight deviation of the parameters from the “sweet spot”. Meanwhile, the low-lying states of this Y-junction being braided now are not necessarily PMMs. It implies that this Y-junction can depict the non-Abelian braiding of different kinds of low-lying modes for different choices of χ ’s and Ω ’s. Specifically, there are four distinct cases based on the magnitudes and the phases of χ_j and Ω_j , which are summarized in TABLE I and will be discussed below in detail.

The braiding operation in this Y-junction is conducted through coupling the three outer sites with the central site in turn [51, 52]. Without loss of generality, we choose swapping the low-lying modes localized at site 2 and site 3 of this Y-junction [see Fig. 1(a)] as an instance. The Y-junction is initialized by setting χ_2 , χ_3 , Ω_2 , and Ω_3 to zero, while setting χ_1 and Ω_1 to finite values. In this way, both site 2 and site 3 become isolated so that each of them contains a zero-energy mode. In the first step of the braiding, χ_2 and Ω_2 are adiabatically increased to finite values, while χ_1 and Ω_1 are adiabatically decreased to zero. Here, we assume the ratios $|\chi_1|/|\Omega_1|$ and $|\chi_2|/|\Omega_2|$ remain constants during the braiding, and the phases $\theta_{\chi_j}, \theta_{\Omega_j}$ also remain unchanged. In this way, the zero-energy mode initially localized at site 2 is adiabatically moved to site 1. In the second step, in the same manner, χ_3 and Ω_3 are both increased to finite values, and χ_2 and Ω_2 are decreased to zero in an adiabatic way so that

the zero-energy mode in site 3 is moved to site 2. In the final step, the braiding is accomplished by increasing χ_1 and Ω_1 to their initial values while decreasing χ_3 and Ω_3 to zero. Such a braiding process corresponds to a closed loop in the parameter space [see Fig. 1(b)].

Non-Abelian braiding of MZMs. We firstly focus on the braiding under the conditions $|\chi_j| = |\Omega_j|$ ($j = 1, 2, 3$), i.e. case I and case II in TABLE I. By decomposing the electron operators d_j into Majorana operators γ_j and $\tilde{\gamma}_j$ ($j = 0, 1, 2, 3$), the original Hamiltonian [Eq. (1)] can be rewritten as [53]:

$$H = -i|\chi_1|\gamma_0\gamma_1 - i|\chi_2|(-\sin\varphi_2\tilde{\gamma}_0 + \cos\varphi_2\gamma_0)\gamma_2 - i|\chi_3|(-\sin\varphi_3\tilde{\gamma}_0 + \cos\varphi_3\gamma_0)\gamma_3. \quad (2)$$

Here, as we have stated before, $\varphi_2 \equiv (\theta_{\chi_2} + \theta_{\Omega_2} - \theta_{\chi_1} - \theta_{\Omega_1})/2$ and $\varphi_3 \equiv (\theta_{\chi_3} + \theta_{\Omega_3} - \theta_{\chi_1} - \theta_{\Omega_1})/2$ are two phase constants (θ_{χ_j} and θ_{Ω_j} remain unchanged during the braiding) that cannot be absorbed even after gauge transformation [53]. This Majorana Hamiltonian [Eq. (2)] can be schematically presented by Fig. 2(a). Specifically, we consider the parity-even subspace spanned by six MZMs $\gamma_0, \gamma_1, \gamma_2, \gamma_3, \tilde{\gamma}_0$, and $\tilde{\gamma}_1$ [dashed box in Fig. 2(a)], because fermion parity is conserved here and the Hamiltonian in the parity-even subspace is identical to that in the parity-odd subspace (up to a constant) [53]. It is worth noting that though $\tilde{\gamma}_1$ is isolated from the other MZMs, it is still intentionally considered to ensure that the dimension of the Fock space is an integer.

In the case I of TABLE I that $\varphi_2, \varphi_3 = 0$, the two-fold degenerate negative-energy states are gapped from the two-fold degenerate positive-energy states (the gap is denoted by Δ), and these degeneracies are preserved throughout the braiding [see Fig. 2(b)]. In the adiabatic limit, where the braiding time $T \gg 1/\Delta$, it is meaningful to consider only the two-fold degenerate ground state manifold. The Berry phase during the braiding can be evaluated analytically [53], which leads to an evolution operator as $U_{\text{case I}} = \begin{pmatrix} e^{-i\pi/4} & 0 \\ 0 & e^{i\pi/4} \end{pmatrix}$. This is precisely

the Majorana braiding operator [7, 52] as expected, since the ‘‘sweet spot’’ condition is satisfied in this case, ensuring that all the low-lying modes in the system are PMMs.

In the case II of TABLE I that $\varphi_2, \varphi_3 \neq 0$, the two-fold ground-state degeneracy is lifted except for three special parameter points during the braiding [see Fig. 2(c)]. Therefore, in addition to the Berry phase, the dynamic phase part in the evolution operator $U = \hat{P} \exp[\int -iE(t)dt + i\mathbf{A}(\boldsymbol{\lambda}) \cdot d\boldsymbol{\lambda}]$ [54, 55] generally cannot be dropped. Here, \hat{P} represents the time-ordering operator, E is a diagonal matrix corresponding to the eigenenergy spectra, and \mathbf{A} is the Berry connection. Under the adiabatic condition, where $T \gg 1/\Delta$, we could still focus only on the two lowest states with negative energies [see Fig. 2(c)]. The corresponding evolution operator can be evaluated numerically as $U_{\text{case II}} =$

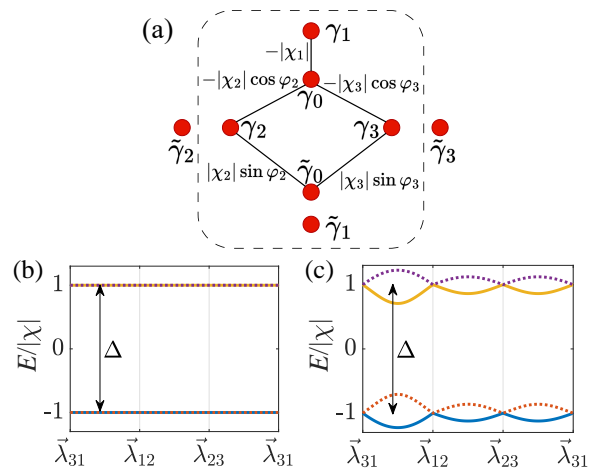


FIG. 2: (a) Schematic representation of the Majorana Hamiltonian [Eq. (2)] under the conditions that $|\chi_j| = |\Omega_j|$. The Fock space we consider is spanned by six MZMs inside the dashed box. (b), (c) The energy spectra during the braiding as (b) Case I in TABLE I that $|\chi_j| = |\Omega_j|$ and $\varphi_2, \varphi_3 = 0$. All the states in (b) are doubly degenerate; (c) Case II in TABLE I that $|\chi_j| = |\Omega_j|$ and $\varphi_2, \varphi_3 \neq 0$ ($\varphi_2 = \pi/6$, and $\varphi_3 = \pi/12$ here for illustration). $|\chi| \equiv \sqrt{|\chi_1|^2 + |\chi_2|^2 + |\chi_3|^2}$ is chosen as the energy unit.

$e^{i\theta} \begin{pmatrix} e^{-i(\pi/4+\delta)} & 0 \\ 0 & e^{i(\pi/4+\delta)} \end{pmatrix}$. Here, the average energy of

these two lowest states contributes a trivial overall dynamic phase θ , while the energy difference between these two lowest states leads to a dynamic phase difference δ [53]. If $\frac{1}{\varphi_2}, \frac{1}{\varphi_3} \gg T \gg \frac{1}{\Delta}$, then this dynamic phase difference δ is relatively small so now the braiding operator comes back to the form of $\text{diag}\{e^{-i\pi/4}, e^{i\pi/4}\}$. It indicates that the geometric phase accumulated remains $\mp\pi/4$ even when $\varphi_2, \varphi_3 \neq 0$, which can be confirmed by analytically evaluating the geometric phase part of the evolution operator $\hat{P} \exp[\int i\mathbf{A}(\boldsymbol{\lambda}) \cdot d\boldsymbol{\lambda}]$ [53]. Otherwise, the dynamic phase dominates when $\frac{1}{\varphi_2}, \frac{1}{\varphi_3} \ll T$, causing the braiding results to oscillate with increasing T [53]. Such results that in addition to the geometric phase of $\mp\pi/4$, an undesired dynamic phase being also involved has been observed in the QD-assisted braiding [39–41, 43]. In fact, as shown in Fig. 2(a), two MZMs γ_2 and γ_3 being braided here are swapped via coupling to both the two Majorana components γ_0 and $\tilde{\gamma}_0$ located at the central site. Therefore, the minimal Kitaev chain here exactly describes the QD-assisted braiding that two MZMs are swapped via a Dirac fermion zero mode.

Non-Abelian braiding of Dirac fermion zero modes. The more intriguing scenario is that even though the equalities $|\chi_j| = |\Omega_j|$ ($j = 1, 2, 3$) are only slightly violated, the low-lying modes being braided are no longer single MZMs, but Majorana pairs. To be specific, under the conditions $|\chi_j| \neq |\Omega_j|$ ($j = 1, 2, 3$), i.e. cases III and IV in TABLE I, the original Hamiltonian [Eq. (1)] in the

Majorana form reads [53]

$$\begin{aligned}
H = & -i \frac{|\chi_1| + |\Omega_1|}{2} \gamma_0 \gamma_1 - i \frac{|\chi_1| - |\Omega_1|}{2} \tilde{\gamma}_0 \tilde{\gamma}_1 \\
& - i \cos \varphi_2 \left(\frac{|\chi_2| + |\Omega_2|}{2} \gamma_0 \gamma_2 + \frac{|\chi_2| - |\Omega_2|}{2} \tilde{\gamma}_0 \tilde{\gamma}_2 \right) \\
& - i \cos \varphi_3 \left(\frac{|\chi_3| + |\Omega_3|}{2} \gamma_0 \gamma_3 + \frac{|\chi_3| - |\Omega_3|}{2} \tilde{\gamma}_0 \tilde{\gamma}_3 \right) \\
& + i \sin \varphi_2 \left(\frac{|\chi_2| + |\Omega_2|}{2} \tilde{\gamma}_0 \gamma_2 - \frac{|\chi_2| - |\Omega_2|}{2} \gamma_0 \tilde{\gamma}_2 \right) \\
& + i \sin \varphi_3 \left(\frac{|\chi_3| + |\Omega_3|}{2} \tilde{\gamma}_0 \gamma_3 - \frac{|\chi_3| - |\Omega_3|}{2} \gamma_0 \tilde{\gamma}_3 \right). \quad (3)
\end{aligned}$$

One can notice that for case III in TABLE I that $\varphi_2 = \varphi_3 = 0$, the cross-coupling terms like $i\gamma_i\tilde{\gamma}_j$ vanish. In this way, a unitary symmetry \mathcal{R} defined as $\mathcal{R}_{ij}i\gamma_i\tilde{\gamma}_j\mathcal{R}_{ij}^{-1} = -i\gamma_i\tilde{\gamma}_j$ is preserved [30], and all these MZMs are separated into two sets as shown in Fig. 3(a). According to the braiding protocol introduced above, these two independent sets of MZMs $\{\gamma_i\}$ and $\{\tilde{\gamma}_i\}$ are braided simultaneously. It is worth noticing that γ_i and $\tilde{\gamma}_i$ are spatially fully-overlapped. Therefore, the low-lying modes being braided here are actually fully-overlapped Majorana pairs respecting local unitary symmetry \mathcal{R} . Then each Majorana pair as a whole is actually Dirac fermion zero mode [30, 31, 56] that the corresponding braiding properties can be constructed from the Majorana ones.

In the adiabatic limit $T \gg \frac{1}{w}, \frac{1}{\Delta}$ [w is the (average) energy difference between the lowest two-fold states and the second lowest two-fold states, see Fig. 3(c)], the Berry phase for the lowest two-fold states turns out to be the projection of the tensor product of the Majorana one's into the parity-even subspace as $\hat{\mathbb{P}}_{\text{even}}[\text{diag}\{e^{-i\pi/4}, e^{i\pi/4}\} \otimes \text{diag}\{e^{-i\pi/4}, e^{i\pi/4}\}] = \text{diag}\{-i, i\}$. Similarly, the Berry phase for the second lowest two-fold states is $\hat{\mathbb{P}}_{\text{even}}[\text{diag}\{e^{-i\pi/4}, e^{i\pi/4}\} \otimes \text{diag}\{e^{i\pi/4}, e^{-i\pi/4}\}] = \text{diag}\{1, 1\}$ [53]. In addition to this, the dynamic phases also contribute when $T \gg \frac{1}{w}, \frac{1}{\Delta}$, and hence the braiding operator reads $U_{\text{case III}} = e^{i\theta} \left[e^{-i\delta} \begin{pmatrix} -i & 0 \\ 0 & i \end{pmatrix} \oplus e^{i\delta} \begin{pmatrix} 1 & 0 \\ 0 & 1 \end{pmatrix} \right]$. Here, θ (δ) are the dynamic phases corresponding to the average energy of (energy difference between) the lowest and second lowest two-fold degenerate states.

By contrast, for $1/w \gg T \gg 1/\Delta$, the dynamic phase of the four lowest states only contributes a trivial overall phase and can be dropped. Moreover, the Berry phase for the Majorana set $\{\tilde{\gamma}_j\}$ now reduces to an identity $I_{4 \times 4}$ since $\tilde{\gamma}_j$'s are braided in the non-adiabatic limit $1/w \gg T$ [55]. Therefore, in this case, the braiding operator is obtained by projecting the tensor product $\text{diag}\{e^{-i\pi/4}, e^{i\pi/4}\} \otimes I_{4 \times 4}$ into the parity-even subspace, giving $U_{\text{case III}} = \text{diag}\{e^{-i\pi/4}, e^{-i\pi/4}, e^{i\pi/4}, e^{i\pi/4}\}$ [53].

Finally, for case IV in TABLE I that $\varphi_2, \varphi_3 \neq 0$, the unitary symmetry \mathcal{R} is broken and the two sets of MZMs $\{\gamma_i\}$ and $\{\tilde{\gamma}_i\}$ are coupled via the cross-coupling

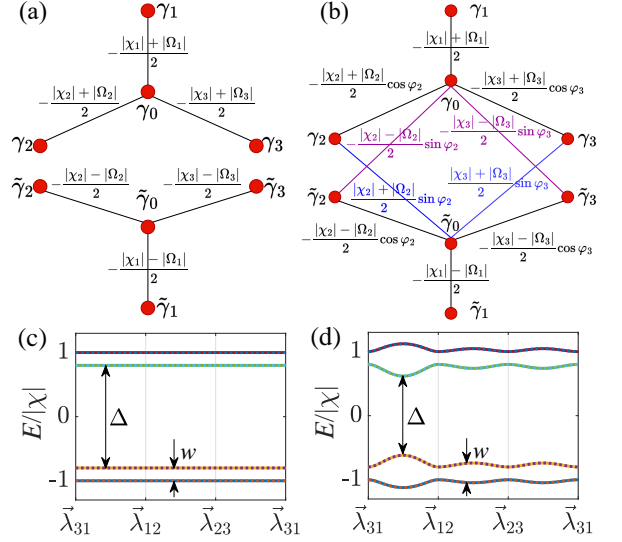


FIG. 3: (a), (b) Schematic representation of the Majorana Hamiltonian [Eq. (3)] under the conditions of (a) Case III in TABLE I; and (b) Case IV in TABLE I. (c), (d) The energy spectra during the braiding as (c) Case III that $|\chi_j| \neq |\Omega_j|$ and $\varphi_2, \varphi_3 = 0$ ($|\Omega_i|/|\chi_i| = 0.8$ here for illustration); and (d) Case IV that $|\chi_j| \neq |\Omega_j|$ and $\varphi_2, \varphi_3 \neq 0$ ($|\Omega_i|/|\chi_i| = 0.8$, $\varphi_2 = \pi/6$, and $\varphi_3 = \pi/12$ here for illustration). The energy unit $|\chi| \equiv \sqrt{|\chi_1|^2 + |\chi_2|^2 + |\chi_3|^2}$, and all the states in (c) and (d) are doubly degenerate.

terms [see Fig. 3(b)]. The energy spectra in Fig. 3(d) shows that all the two-fold degeneracies are still preserved, while the energies of these degenerate states vary during the braiding. Through numerical calculation [53], we have confirmed that the Berry phase accumulated in case IV is exactly the same as the one in case III (up to a gauge transform). This is in analogy with the consequence stated above that the Berry phase is the same for case II and case I. The difference lies in that now the dynamic phases $\theta \mp \delta$ are φ_2 , φ_3 , and $|\Omega_j|/|\chi_j|$ -dependent since the energy during the braiding vary with φ_2 , φ_3 , and $|\Omega_j|/|\chi_j|$. Meanwhile, the braiding results still exhibit an oscillation with increasing T [53]. Moreover, the (average) energy difference w between the two-fold ground states and the second-lowest two-fold states also increases with φ_2 , φ_3 , and $||\chi_j| - |\Omega_j||$. In this way, the $1/w \gg T \gg 1/\Delta$ condition can no longer be satisfied when φ_2 , φ_3 , or $||\chi_j| - |\Omega_j||$ is significantly non-zero. As a result, an additional dynamic phase is always accumulated alongside the geometric phase, providing a clear signature of the symmetry-breaking effect [31, 56, 57] on the braiding of Dirac fermion zero modes.

Discussions. The minimal Kitaev chain model is experimentally feasible, in ultracold atom systems for instance, especially for $|\Omega_j| = 0 \neq |\chi_j|$, as the complexity of pairing term is circumvented. In this case, the low-lying modes are Dirac fermion modes with unitary symmetry preserved (case III) or broken (case IV),

other than MZMs. In this condition, the Hamiltonian in Eq. (1) can be engineered by utilizing the internal degree of freedom of atoms. Taking ^{171}Yb fermions as an example, the four braiding modes correspond to the atomic spin states, $^1\text{S}_0|F = 1/2, m_F = \pm 1/2\rangle$, and $^3\text{P}_0|F = 1/2, m_F = \pm 1/2\rangle$, which have significantly long lifetime. The tunnelings among the four fermion modes are highly controllable by manipulating Raman and clock transitions [58].

Acknowledgements. This work was financially supported by the Innovation Program for Quantum Science and Technology (Grant No. 2021ZD0302400 and No. 2021ZD0302000), the National Natural Science Foundation of China (Grant No. 12304194, No. 12425401 and No. 12261160368), National Key Research and Development Program of China (2021YFA1400900), and by Shanghai Municipal Science and Technology (Grant No. 24DP2600100).

* These authors equally contribute to this article.

† xiongjunliu@pku.edu.cn

‡ xcxie@fudan.edu.cn

§ yjiawu@fudan.edu.cn

- [1] F. Wilczek, Phys. Rev. Lett. **49**, 957 (1982).
- [2] R. B. Laughlin, Phys. Rev. Lett. **50**, 1395 (1983).
- [3] D. C. Tsui, H. L. Stormer, and A. C. Gossard, Phys. Rev. Lett. **48**, 1559 (1982).
- [4] R. Willett, J. P. Eisenstein, H. L. Stormer, D. C. Tsui, A. C. Gossard, and J. H. English, Phys. Rev. Lett. **59**, 1776 (1987).
- [5] G. Moore and N. Read, Nuclear Physics B **360**, 362 (1991).
- [6] X. G. Wen, Phys. Rev. Lett. **66**, 802 (1991).
- [7] D. A. Ivanov, Phys. Rev. Lett. **86**, 268 (2001).
- [8] A. Y. Kitaev, Physics-uspekhi **44**, 131 (2001).
- [9] A. Y. Kitaev, Annals of physics **303**, 2 (2003).
- [10] C. Nayak, S. H. Simon, A. Stern, M. Freedman, and S. Das Sarma, Rev. Mod. Phys. **80**, 1083 (2008).
- [11] L. Fu and C. L. Kane, Phys. Rev. Lett. **100**, 096407 (2008).
- [12] V. Mourik, K. Zuo, S. M. Frolov, S. Plissard, E. P. Bakkers, and L. P. Kouwenhoven, Science **336**, 1003 (2012).
- [13] A. Das, Y. Ronen, Y. Most, Y. Oreg, M. Heiblum, and H. Shtrikman, Nature Physics **8**, 887 (2012).
- [14] Z. Cao, S. Chen, G. Zhang, and D. E. Liu, Science China Physics, Mechanics & Astronomy **66**, 267003 (2023).
- [15] S. Nadj-Perge, I. K. Drozdov, J. Li, H. Chen, S. Jeon, J. Seo, A. H. MacDonald, B. A. Bernevig, and A. Yazdani, Science **346**, 602 (2014).
- [16] H.-H. Sun, K.-W. Zhang, L.-H. Hu, C. Li, G.-Y. Wang, H.-Y. Ma, Z.-A. Xu, C.-L. Gao, D.-D. Guan, Y.-Y. Li, et al., Phys. Rev. Lett. **116**, 257003 (2016).
- [17] D. Wang, L. Kong, P. Fan, H. Chen, S. Zhu, W. Liu, L. Cao, Y. Sun, S. Du, J. Schneeloch, et al., Science **362**, 333 (2018).
- [18] P. Zhang, K. Yaji, T. Hashimoto, Y. Ota, T. Kondo, K. Okazaki, Z. Wang, J. Wen, G. Gu, H. Ding, et al., Science **360**, 182 (2018).
- [19] W. Liu and H. Ding, Science China Physics, Mechanics & Astronomy **66**, 267002 (2023).
- [20] W. Ji and X.-G. Wen, Phys. Rev. Lett. **120**, 107002 (2018).
- [21] J. Liu, A. C. Potter, K. T. Law, and P. A. Lee, Phys. Rev. Lett. **109**, 267002 (2012).
- [22] C.-X. Liu, J. D. Sau, T. D. Stanescu, and S. Das Sarma, Phys. Rev. B **96**, 075161 (2017).
- [23] C. L. M. Wong and K. T. Law, Phys. Rev. B **86**, 184516 (2012).
- [24] F. Zhang, C. L. Kane, and E. J. Mele, Phys. Rev. Lett. **111**, 056402 (2013).
- [25] X.-J. Liu, C. L. M. Wong, and K. T. Law, Phys. Rev. X **4**, 021018 (2014).
- [26] K. Wölms, A. Stern, and K. Flensberg, Phys. Rev. Lett. **113**, 246401 (2014).
- [27] K. Wölms, A. Stern, and K. Flensberg, Phys. Rev. B **93**, 045417 (2016).
- [28] P. Gao, Y.-P. He, and X.-J. Liu, Phys. Rev. B **94**, 224509 (2016).
- [29] C. Schrade and L. Fu, Phys. Rev. Lett. **129**, 227002 (2022).
- [30] J.-S. Hong, T.-F. J. Poon, L. Zhang, and X.-J. Liu, Phys. Rev. B **105**, 024503 (2022).
- [31] Y. Wu, H. Jiang, J. Liu, H. Liu, and X. C. Xie, Phys. Rev. Lett. **125**, 036801 (2020).
- [32] S. Yasui, K. Itakura, and M. Nitta, Nuclear Physics B **859**, 261 (2012).
- [33] W.-Y. Shan, J. Lu, H.-Z. Lu, and S.-Q. Shen, Phys. Rev. B **84**, 035307 (2011).
- [34] R. Jackiw and C. Rebbi, Phys. Rev. D **13**, 3398 (1976).
- [35] W. P. Su, J. R. Schrieffer, and A. J. Heeger, Phys. Rev. Lett. **42**, 1698 (1979).
- [36] J. Klinovaja and D. Loss, Phys. Rev. Lett. **110**, 126402 (2013).
- [37] J. Klinovaja and D. Loss, Phys. Rev. B **92**, 121410 (2015).
- [38] P. Boross, J. K. Asbóth, G. Széchenyi, L. Oroszlány, and A. Pályi, Phys. Rev. B **100**, 045414 (2019).
- [39] K. Flensberg, Phys. Rev. Lett. **106**, 090503 (2011).
- [40] J. Liu, W. Chen, M. Gong, Y. Wu, and X. C. Xie, Science China Physics, Mechanics & Astronomy **64**, 117811 (2021).
- [41] M. Gong, Y. Wu, H. Jiang, J. Liu, and X. C. Xie, Phys. Rev. B **105**, 014507 (2022).
- [42] S. Krøjer, R. Seoane Souto, and K. Flensberg, Phys. Rev. B **105**, 045425 (2022).
- [43] L. Xu, J. Bai, W. Feng, and X.-Q. Li, Phys. Rev. B **108**, 115411 (2023).
- [44] M. Leijnse and K. Flensberg, Phys. Rev. B **86**, 134528 (2012).
- [45] A. Tsintzis, R. Souto, K. Flensberg, et al., PRX Quantum **5**, 010323 (2024).
- [46] J.-S. Hong, S.-Q. Zhang, X. Liu, and X.-J. Liu, arXiv preprint arXiv:2403.09602 (2024).
- [47] P. Ghosh, J. D. Sau, S. Tewari, and S. Das Sarma, Phys. Rev. B **82**, 184525 (2010).
- [48] R. M. Lutchyn, T. D. Stanescu, and S. Das Sarma, Phys. Rev. Lett. **106**, 127001 (2011).
- [49] B. Zhou and S.-Q. Shen, Phys. Rev. B **84**, 054532 (2011).
- [50] J. Alicea, Y. Oreg, G. Refael, F. Von Oppen, and M. P. Fisher, Nature Physics **7**, 412 (2011).
- [51] J. D. Sau, D. J. Clarke, and S. Tewari, Phys. Rev. B **84**,

- 094505 (2011).
- [52] F. von Oppen, Y. Peng, and F. Pientka, *Topological Aspects of Condensed Matter Physics* **103**, 387 (2017).
- [53] See Supplementary Materials for the derivation of the Hamiltonian in the Majorana basis, the analytical evaluation of the non-Abelian Berry phases accumulated, and the numerical calculation of the dynamic phases.
- [54] F. Wilczek and A. Zee, *Phys. Rev. Lett.* **52**, 2111 (1984).
- [55] M.-C. Chang, Lecture notes on topological insulators (2021), URL <https://phy.ntnu.edu.tw/~changmc/Teach/Topo/latex/2020/02.pdf>.
- [56] Y. Wu, J. Liu, and X. C. Xie, *Science China Physics, Mechanics & Astronomy* **66**, 267004 (2023).
- [57] Y. Wu, H. Liu, J. Liu, H. Jiang, and X. C. Xie, *National Science Review* **7**, 572 (2020).
- [58] A. Jenkins, J. W. Lis, A. Senoo, W. F. McGrew, and A. M. Kaufman, *Phys. Rev. X* **12**, 021027 (2022).